Effects of hydrophobic surface on skin-friction drag

Taegee Min and John Kim
Department of Mechanical and Aerospace Engineering, University of California, Los Angeles, California 90095-1597

(Received 2 March 2004; accepted 5 April 2004; published online 25 May 2004)

Effects of hydrophobic surface on skin-friction drag are investigated through direct numerical simulations of a turbulent channel flow. Hydrophobic surface is represented by a slip-boundary condition on the surface. When a slip-boundary condition is used in the streamwise direction, the skin-friction drag decreases and turbulence intensities and turbulence structures, near-wall streamwise vortices in particular, are significantly weakened. When a slip-boundary condition is used in the spanwise direction, on the other hand, the drag is increased. It is found that near-wall turbulence structures are modified differently, resulting in drag increase. It is also found that the slip length must be greater than a certain value in order to have a noticeable effect on turbulence. An important implication of the present finding is that drag reduction in turbulent boundary layers is unlikely with hydrophobic surface with its slip length on the order of a submicron scale. © *2004 American Institute of Physics.* [DOI: 10.1063/1.1755723]

Recent advancement in nano- and microtechnology has opened up the possibility of using nano- and microdevices in a wide variety of applications. In nano- and microfluidic devices, surface properties play a predominant role. One surface property that has received much attention lately is the hydrophobic or hydrophilic nature of surfaces fabricated by using nano- or microtechnology. It has been reported, for example, that the slip velocity on hydrophobic surfaces results in significant drag reduction in microchannel flows.[1,2]

On a totally different front, the fouling of a ship's surface by barnacles and seaweed is a major problem in the ship-building industry, because the rough surface in general increases the drag, resulting in higher fuel consumption. In order to prevent the fouling, toxic paints have been used, but their usage has been phased out due to environmental reasons. Some investigators have been developing nontoxic self-cleaning coatings with hydrophobic or hydrophilic property by utilizing nanotechnology.[3] However, the effect of such surface on the skin-friction drag in large-scale flows, such as turbulent flows around a ship, is unknown.

The objective of the present study is to examine the question of whether such a hydrophobic surface with its slip length (to be defined below) typically on the order of submicron meters, can also reduce the skin-friction drag in turbulent flows in much larger devices.

In this Letter, we shall use u, v and w to denote, respectively, the velocity component in the streamwise (x), wall-normal (y) and spanwise (w) directions. All quantities are normalized by the wall-shear velocity, u_τ, and the channel half width, δ, unless stated otherwise. The superscript $^+$ denotes flow variables normalized by u_τ and the kinematic viscosity, ν.

Experimental studies[1,2,4] have shown that flows with hydrophobic surface can be analyzed by the Navier–Stokes equations with a slip-boundary condition. In the present study, direct numerical simulations of a turbulent channel flow with hydrophobic surface are performed using the following slip-boundary condition:

$$u_s = L_s \left.\frac{\partial u}{\partial y}\right|_{\text{wall}}, \quad w_s = L_s \left.\frac{\partial w}{\partial y}\right|_{\text{wall}}, \tag{1}$$

where u_s and w_s denote the streamwise and spanwise slip velocity, respectively, and L_s denotes the slip length. The slip length L_s generally depends on the shear rate, $\partial u/\partial y|_{\text{wall}}$ and $\partial w/\partial y|_{\text{wall}}$ (Choi *et al.*[2]). In the present study, however, the slip length is assumed to be independent of the shear rate, which is valid for moderate shear rates.[5]

A semi-implicit, fractional step method similar to that used by Kim and Moin[6] is used to solve the Navier–Stokes equations for incompressible flows. All spatial derivatives are discretized using second-order central difference schemes, while a third-order Runge–Kutta scheme and Crank–Nicolson scheme are used, respectively, for time advancement of the nonlinear and viscous terms. Simulations are conducted at $\mathrm{Re}=U_c\delta/\nu=4200$ or $\mathrm{Re}_\tau=u_{\tau_0}\delta/\nu\simeq 180$, where U_c and δ, respectively, denote the centerline velocity and the channel half height, and u_{τ_0} denotes the wall-shear velocity for regular (i.e., no-slip walls) channel flow. The computational domain of $7\delta\times 2\delta\times 3.5\delta$ is used in the streamwise, wall-normal and spanwise directions, respectively, with $128\times 129\times 128$ grids ($\Delta x^+\simeq 10$, $\Delta y^+_{\min}\simeq 0.3$, $\Delta z^+\simeq 5$). Examinations of the computed spectra at various wall-normal indications revealed that this resolution was adequate.

In order to delineate the effect of the streamwise and spanwise slip-boundary conditions separately, three different cases are performed: (1) Case 1, streamwise slip only ($u_s\neq 0$, $w_s=0$), (2) Case 2, spanwise slip only ($u_s=0$, $w_s\neq 0$); and (3) Case 3, slip in both directions ($u_s\neq 0$, $w_s\neq 0$). A constant mass flow rate is maintained for all cases, and the resulting mean pressure gradient is monitored to in-

TABLE I. Drag and mean slip velocity variation with slip length. Here, L_s^+ denotes the slip length normalized by the wall shear velocity of no-slip walls u_{τ_0}, and u_s^+ denotes the mean slip velocity normalized by the actual wall shear velocity u_τ.

		Case 1		Case 2	Case 3	
L_s	L_s^+	u_s^+	DR	DR	u_s^+	DR
0.0002	0.036	0.035	0	0	0.035	0
0.0005	0.089	0.088	−1	+1	0.089	−1
0.001	0.178	0.176	−2	+2	0.177	−2
0.002	0.357	0.349	−5	+3	0.355	−1
0.005	0.891	0.845	−10	+8	0.877	−3
0.01	1.783	1.618	−18	+16	1.707	−8
0.02	3.566	3.006	−29	+26	3.238	−17

fer the skin-friction drag. The percentage change in the drag, DR, is defined as

$$DR = \frac{\left(-\frac{d\overline{p}}{dx}\right) - \left(-\frac{d\overline{p}}{dx}\Big|_0\right)}{-\frac{d\overline{p}}{dx}\Big|_0} \times 100, \tag{2}$$

where $-d\overline{p}/dx|_0$ represents the mean pressure gradient with the no-slip boundary condition.

Table I shows the mean skin-friction drag and the mean slip velocity as the slip length varies. It is worth mentioning that the drag in laminar flow decreases with any slip length in the streamwise direction. In turbulent flows, however, the present results show that the slip length, L_s^+ must be larger than 0.2 in order to have noticeable drag reduction. Both the mean slip velocity u_s^+ and the drag reduction are increased as the slip length increases. Note that the mean drag increases when the slip-boundary condition is used in the spanwise direction (Case 2). This result is consistent with that found by Choi *et al.*[7] and Jiménez,[8] who investigated the effect of spanwise slip velocity in a feedback controlled turbulent channel flow. When the slip-boundary condition is used in both directions (Case 3), the reduction is less (than that corresponding to Case 1), indicating that the drag-reducing effect of the streamwise slip is countered by the drag-increasing effect of the spanwise slip. Hahn *et al.*[9] have shown similar results for turbulent channel flow with a permeable wall, which has the same boundary condition as Eq. (1) when the flow inside the permeable wall is negligible.

Figure 1 shows the mean streamwise velocity profiles normalized by the wall-shear velocity u_τ. The results of Kim *et al.*[10] are also shown for comparison. As expected, there is an upward shift for drag-reduced cases and a downward shift for drag-increased cases. In order to delineate the simple effect of nonzero mean slip velocity u_s^+, we plot $u^+ - u_s^+$ in Fig. 2. Plotted in this way, all velocity profiles from Case 1 collapse into one, which then corresponds to the regular channel flow. Case 3 shows a mixed trend of the streamwise and spanwise slip: that is, profiles collapse in the viscous sublayer and show a downward shift in buffer and log layers. Note that these results are quite different from that observed in other drag-reducing flows, such channel flow

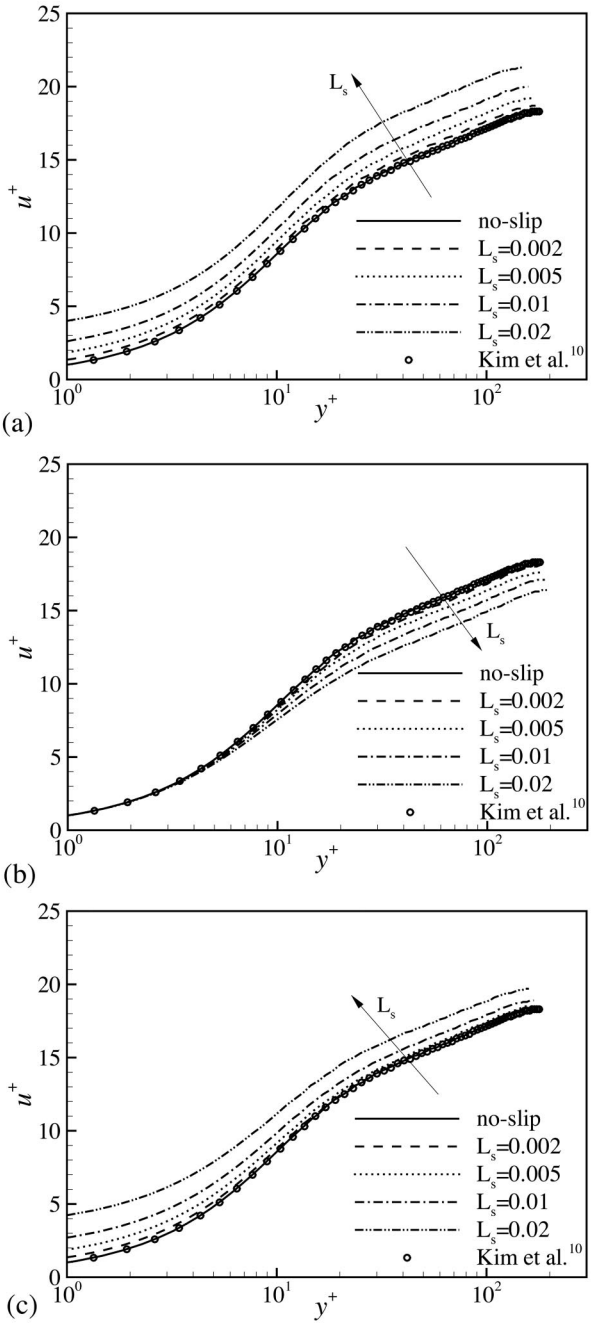

FIG. 1. Mean velocity profiles, u^+: (a) Case 1, streamwise slip; (b) Case 2, spanwise slip; (c) Case 3, combined slip.

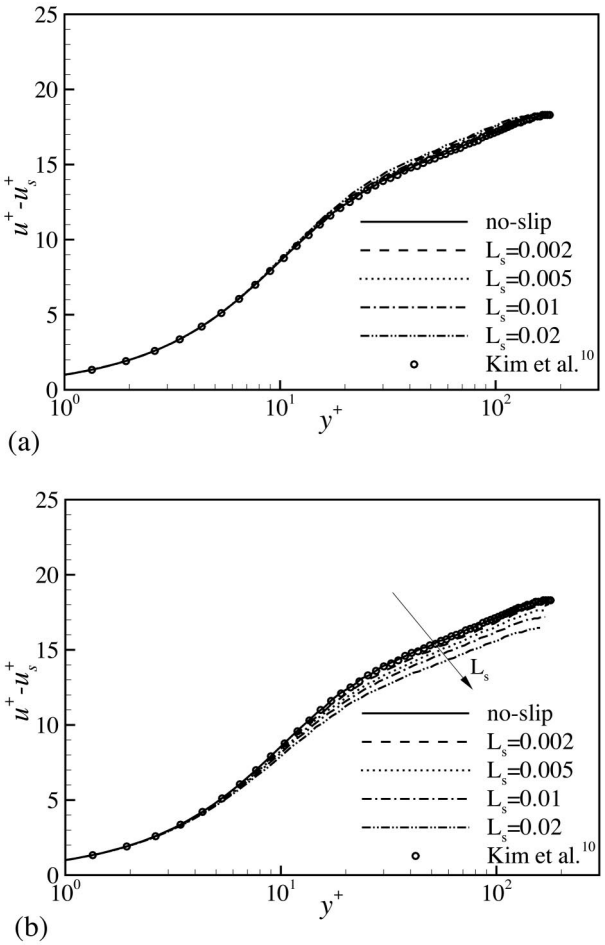

FIG. 2. Mean velocity profiles, $u^+ - u_s^+$: (a) Case 1; (b) Case 3.

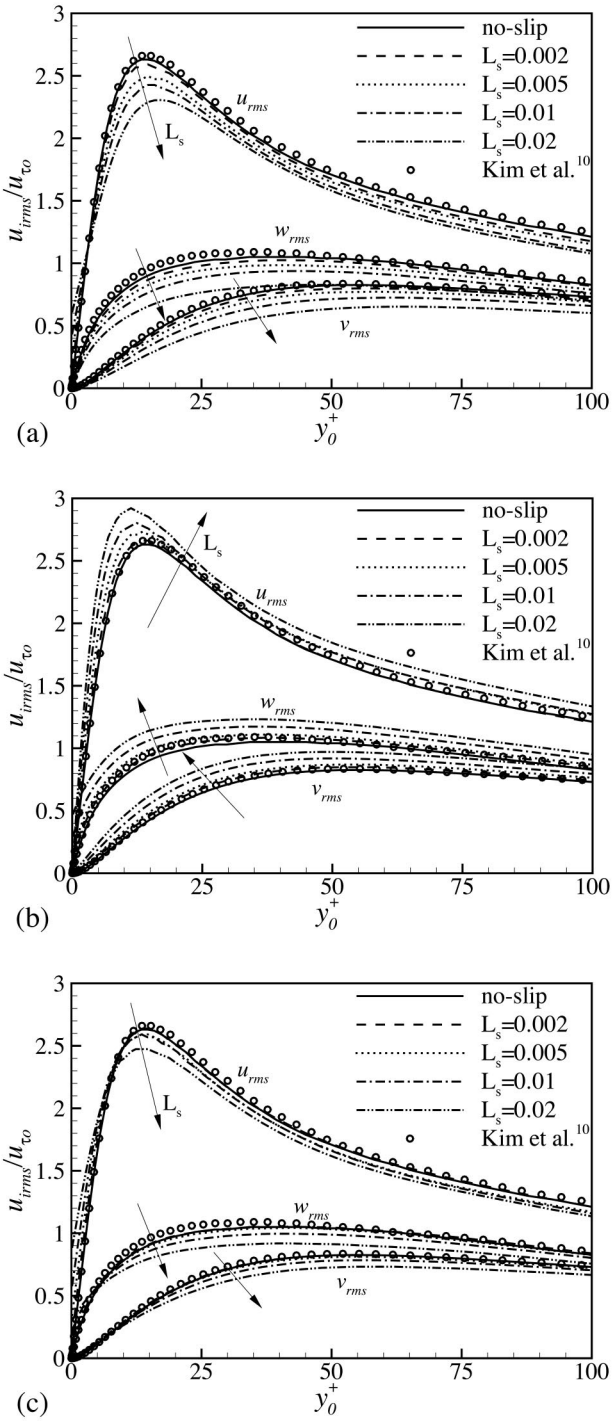

FIG. 3. The rms velocity fluctuations normalized by u_{τ_0}: (a) Case 1; (b) Case 2; (c) Case 3.

with active blowing/suction at the wall[7] and channel flow with polymer,[11] where upward shifts in the log-law are observed.

Figure 3 shows the root-mean square (rms) velocity fluctuations normalized by u_{τ_0}. The rms fluctuations are decreased significantly for Cases 1 and 3 (more so with larger L_s), whereas the rms fluctuations are increased for Case 2. Note that the increase of u_{rms} and w_{rms} very close to the wall for Cases 1 and 3 is due to fluctuations of the slip velocities u_s and w_s.

Contours of streamwise vorticity in y-z are shown in Fig. 4. It is apparent from Fig. 4 that near-wall streamwise vortices are significantly weakened for Cases 1 and 3 (more so for Case 1, given the same slip length). It is also observed (not shown here) that the strength and coherence (as visualized by contours of wall-normal vorticity) of near-wall streaky structures are significantly reduced for Cases 1 and 3, whereas they are increased for Case 2.

We have seen that the slip velocity in the streamwise and spanwise directions affects the near-wall turbulence field quite differently, resulting in drag reduction with the former and drag increase with the latter. Different effects are described in a schematic representation shown in Fig. 5. The reduction due to the streamwise slip is straightforward. As shown in Fig. 5(a), wall-shear stress is smaller with a streamwise slip, and drag reduction is a direct consequence. For the case of spanwise slip, however, its effect is indirect. The strength of near-wall streamwise vortices are enhanced with a spanwise slip as shown in Fig. 5(b), which in turn results in a drag increase. This situation is similar to in-phase blowing and suction used by Choi *et al.*,[7] which enhances the strength of the streamwise vortices, and as a consequence, increases the skin-friction drag.

In this Letter, we have shown that surface boundary condition, such as hydrophobic or hydrophilic, plays a signifi-

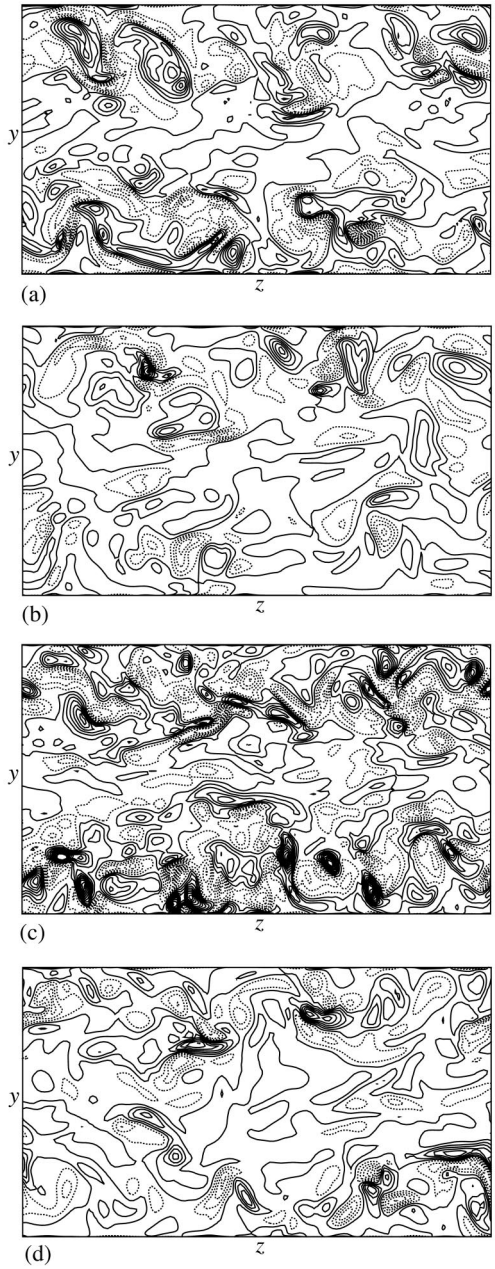

FIG. 4. Contours of streamwise vorticity in y-z plane for $L_s=0.02$: (a) regular channel; (b) Case 1; (c) Case 2; (d) Case 3. Contour levels are from -100 to 100 in increments of 10.

cant role in determining the nature of near-wall turbulence. Streamwise slip can reduce the skin-friction drag, whereas spanwise slip can increase the drag. The latter result is consistent with that observed by Choi *et al.*[7] and Jiménez.[8] With combined slip, the reduction is less due to the adverse effects of spanwise slip. We have also shown that the slip length L_s^+ has to be larger than 0.2 in order to have a noticeable reduction.[12] It is worth noting that for a given hydrophobic surface, the slip length L_s^+ becomes larger for larger skin friction. That is, drag reduction would be greater in case of higher Reynolds number turbulent boundary layers such as ship's surface. At present, a typical slip length for a hydrophobic surface is $10^{-8}\sim10^{-6}$ m,[2] which is much too small

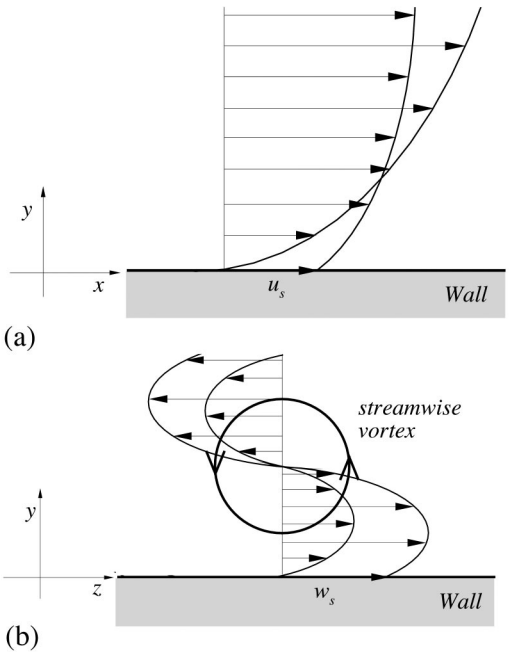

FIG. 5. A schematic representation of drag decrease and increase mechanism: (a) drag decreases with a streamwise slip velocity (x-y plane); (b) drag increases with a spanwise slip velocity (y-z plane).

to have any effect in turbulent flows in a large-scale device. However, the UCLA group[13] has shown recently that they can fabricate a hydrophobic surface with much larger slip length, promising that it is feasible, at least in principle, to achieve skin-friction drag reduction in turbulent boundary layers.

[1] D. C. Tretheway and C. D. Meinhart, "Apparent fluid slip at hydrophobic microchannel walls," Phys. Fluids **14**, L9 (2002).
[2] C. Choi, K. J. A. Westin, and K. S. Breuer, "Apparent slip flows in hydrophilic and hydrophobic microchannels," Phys. Fluids **15**, 2897 (2003).
[3] J. P. Youngblood, L. Andruzzi, C. K. Ober, A. Hexemer, E. J. Kramer, J. A. Callow, J. A. Finlay, and M. E. Callow, "Coating based on side-chain ether-linked poly(ethylene glycol) and fluorocarbon polymers for the control of marine biofouling," Biofouling **19**, 91 (2003).
[4] K. Watanabe, Yanuar, and H. Udagawa, "Drag reduction of Newtonian fluid in a circular pipe with a highly water-repellent wall," J. Fluid Mech. **381**, 225 (1999).
[5] R. Pit, H. Hervet, and L. Léger, "Direct experimental evidence of slip in hexadecane: Solid interfaces," Phys. Rev. Lett. **85**, 980 (2000).
[6] J. Kim and P. Moin, "Application of a fractional-step method to incompressible Navier–Stokes equations," J. Comput. Phys. **59**, 308 (1985).
[7] H. Choi, P. Moin, and J. Kim, "Active turbulence control for drag reduction in wall-bounded flows," J. Fluid Mech. **262**, 75 (1994).
[8] J. Jiménez, "On the structure and control of near wall turbulence," Phys. Fluids **6**, 944 (1994).
[9] S. Hahn, J. Je, and H. Choi, "Direct numerical simulation of turbulent channel flow with permeable walls," J. Fluid Mech. **450**, 259 (2002).
[10] J. Kim, P. Moin, and R. Moser, "Turbulence statistics in fully developed channel flow at low Reynolds number," J. Fluid Mech. **177**, 133 (1987).
[11] T. Min, J. Y. Yoo, H. Choi, and D. D. Joseph, "Drag reduction by polymer additives in a turbulent channel flow," J. Fluid Mech. **486**, 213 (2003).
[12] We have performed a few simulations at $\mathrm{Re}_\tau\simeq400$, which showed the drag reduction was proportional to L_s^+.
[13] J. Kim and C. J. Kim, "Nanostructured surfaces for dramatic drag reduction of flow resistance in droplet-based microfluidics," *Technical Digest, The Fifteenth IEEE International Conference on Micro Electro Mechanical Systems*, Las Vegas, NV, 20–24 January 2002 (IEEE, Piscataway, NJ, 2002), p. 479.